

A Universal and Modular Scaffold for Heparanase Activatable Probes and Drugs

Kelton A. Schleyer,[#] Jun Liu,[#] Zixin Chen, Zhishen Wang, Yuzhao Zhang, Junxiang Zuo, Alberto Jimenez Ybargollin, Hua Guo, and Lina Cui*



Cite This: *Bioconjugate Chem.* 2022, 33, 2290–2298



Read Online

ACCESS |



Metrics & More

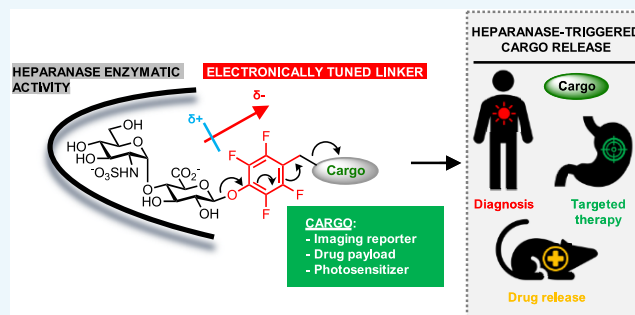


Article Recommendations



Supporting Information

ABSTRACT: Heparanase (HPSE) is an endo- β -glucuronidase involved in extracellular matrix remodeling in rapidly healing tissues, most cancers and inflammation, and viral infection. Its importance as a therapeutic target warrants further study, but such is hampered by a lack of research tools. To expand the toolkits for probing HPSE enzymatic activity, we report the design of a substrate scaffold for HPSE comprised of a disaccharide substrate appended with a linker, capable of carrying cargo until being cleaved by HPSE. Here exemplified as a fluorogenic, coumarin-based imaging probe, this scaffold can potentially expand the availability of HPSE-responsive imaging or drug delivery tools using a variety of imaging moieties or other cargo. We show that electronic tuning of the scaffold provides a robust response to HPSE while simplifying the structural requirements of the attached cargo. Molecular docking and modeling suggest a productive probe/HPSE binding mode. These results further support the hypothesis that the reactivity of these HPSE-responsive probes is predominantly influenced by the electron density of the aglycone. This universal HPSE-activatable scaffold will greatly facilitate future development of HPSE-responsive probes and drugs.



Heparanase (HPSE) is an endo- β -glucuronidase that cleaves the glycosidic bonds of heparan sulfate (HS) chains present in heparan sulfate proteoglycans (HSPG) localized in the extracellular matrix (ECM) and basement membrane.¹ Through this enzymatic activity, HPSE mediates the critical roles HS plays in both the structural integrity of the ECM and in cell–cell signaling through the release of cytokines, chemokines, and growth factors involved in biological and pathological processes.^{2–4} Under normal physiological conditions, high levels of HPSE are found in the placenta and blood-borne cells such as platelets, neutrophils, mast cells, and lymphocytes.³ Notably, HPSE is overexpressed in most types of tumors,^{1,5} and its enzymatic activity is correlated with tumor metastasis, angiogenesis, and poor postsurgical survival.⁶ HPSE is also associated with inflammatory disorders^{3,7} and autoimmune diseases,⁸ and recent studies have elaborated its role in the infection cycle of viruses, including SARS-CoV-2.⁹ These diverse and critical influences have led HPSE to be considered a promising pharmacological target for the diagnosis and treatment of multiple diseases.^{3,4,10}

Since its discovery and the elucidation of its involvement in various pathological conditions, HPSE has met with growing interest and the concomitant development of new tools for its examination.¹¹ Historically, heparan sulfate polysaccharides were used to develop radioisotope-based^{14,15} or fluorescent¹² assays; however these assays inherently suffer from the

heterogeneity of the polysaccharides that can be a result of varying sources and manufacturing,^{13,14} prohibiting the advancement of targeting heparanase in diagnosis and disease treatment. The development of small-molecule HPSE probes has long been considered the “gold standard” of HPSE detection¹³ by providing simple, sensitive, and rapid methods to detect and quantify HPSE activity. This gold standard appeared feasible when the smallest substrate sequence of HPSE was identified to be a trisaccharide,¹⁵ though still challenging considering the inherent complexity of heparan sulfate oligosaccharide synthesis.¹⁶ Considering the typical mechanisms used in turn-on probes for enzyme activity,¹⁷ the most attractive HPSE probe would use the disaccharide on the nonreducing end of this reported trisaccharide, paired with a releasable reporter, a conclusion supported by a disaccharide glycosyl fluoride NMR-based substrate reported for HPSE.¹⁸ However, the exclusion of the third residue in the trisaccharide substrate sequence, which is the acceptor of the glycosidic linkage cleaved by HPSE, precludes significant interactions

Received: September 19, 2022

Revised: November 2, 2022

Published: November 8, 2022



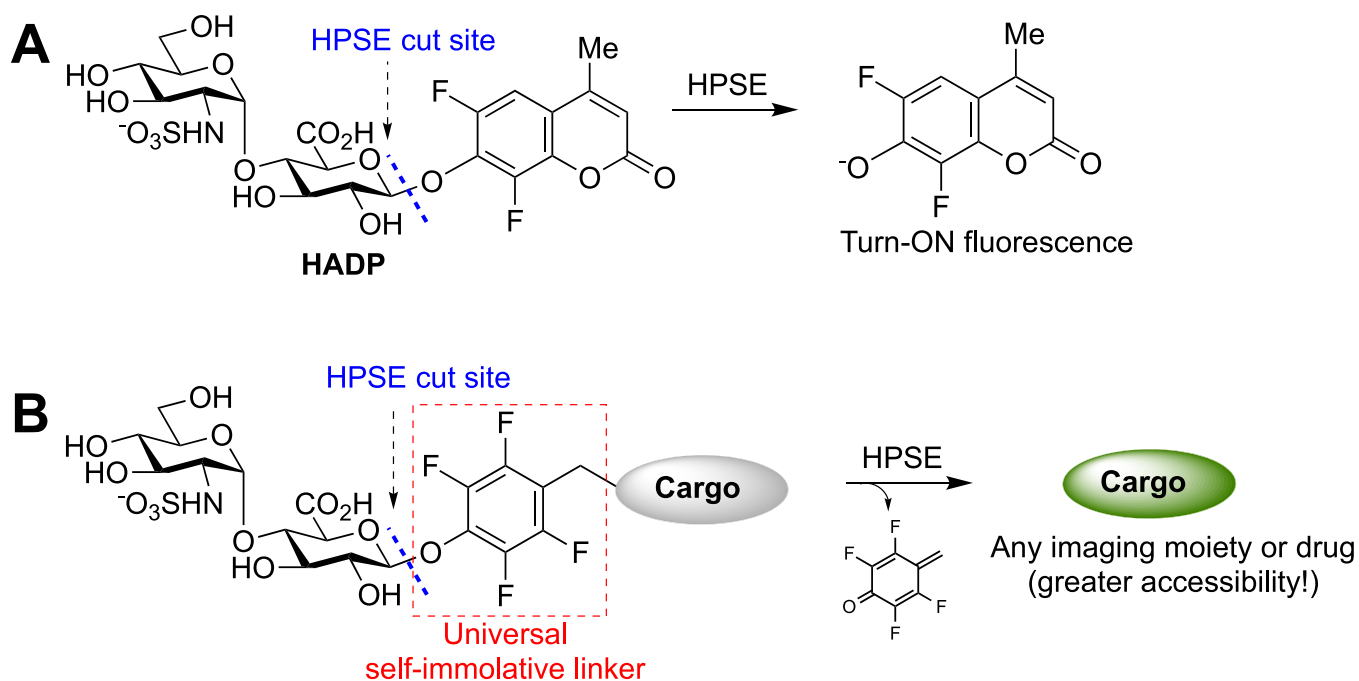
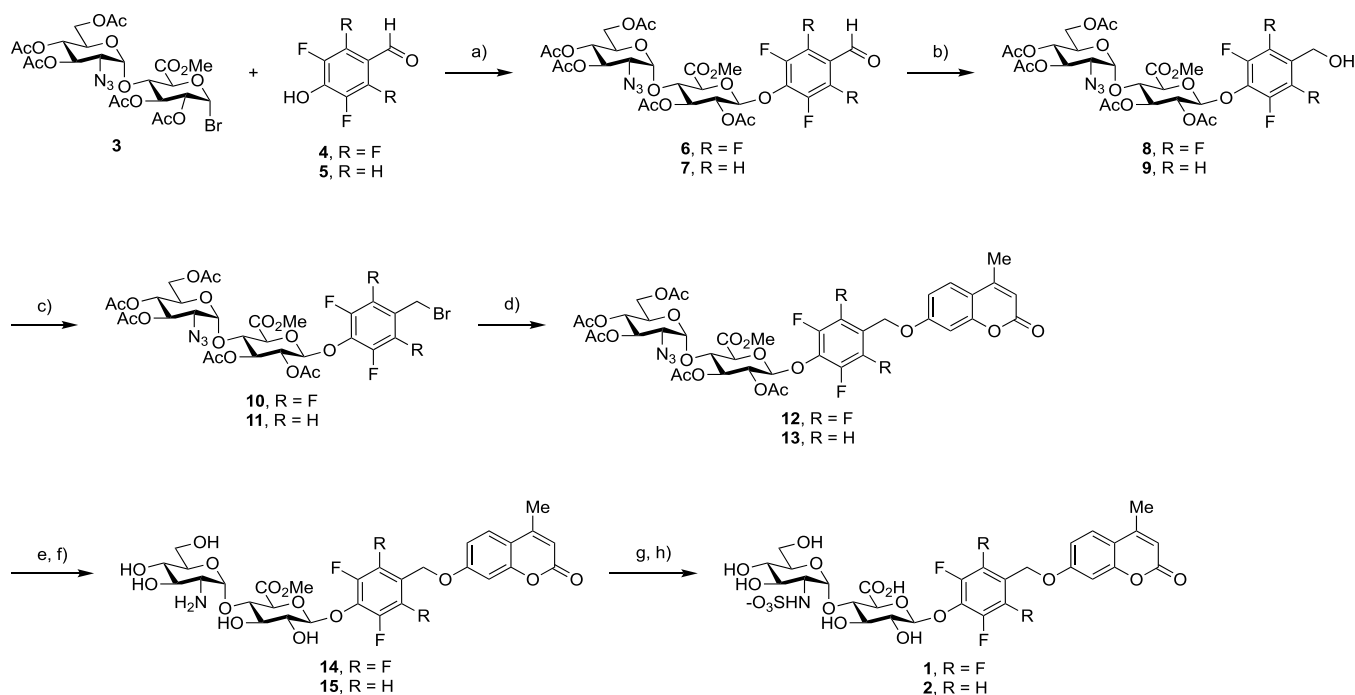


Figure 1. (A) Previous HPSE probe, HADP, tuned by the incorporation of an *o,o*-difluoro motif on the leaving group. While effective, this strategy is incompatible with some desired leaving groups (fluorophores, drug payload, etc.) (B) This work presents a universal scaffold for HPSE probes, utilizing a self-immolative linker that enables the use of standard leaving groups and reporters.

Scheme 1. Synthetic Scheme for Candidate Probes 1 and 2^a



^aReagents and conditions: (a) Ag₂O, MeCN (dry), r.t., OVN, 54% (6) or 77% (7); (b) NaBH₄, DCM/MeOH (1/5), r.t., 20 min, 64% (8) or 77% (9); (c) PPh₃, CBr₄, DCM (dry), r.t., 1 h, 99% (10) or 98% (11); (d) 4-MU, K₂CO₃, DMF, r.t., 16 h, 50% (12) or 25% (13); (e) NaOMe, MeOH, pH 11, r.t., 2 h; (f) PMe₃, MeOH, rt, 1.5 h; 53% (14) or 55% (15) over two steps; (g) NaOH (pH 9), H₂O, rt, 1.5 h; (h) Py-SO₃, NaOH (pH 11), H₂O, rt, 6 h, 80% (1) or 65% (2) by HPLC, over two steps.

between the substrate and active site which contribute to enzymatic processing, thus significantly compromising the activity of the probe.¹⁹

Overcoming this design challenge, we achieved the gold standard of HPSE probes by developing the first structurally

defined ultrasensitive fluorogenic probe HADP (heparanase activatable disaccharide probe, Figure 1A) for single-step detection of HPSE activity with high selectivity and sensitivity.²⁰ HADP has enabled a convenient and efficient high-throughput screen for novel HPSE inhibitors.²⁰ As

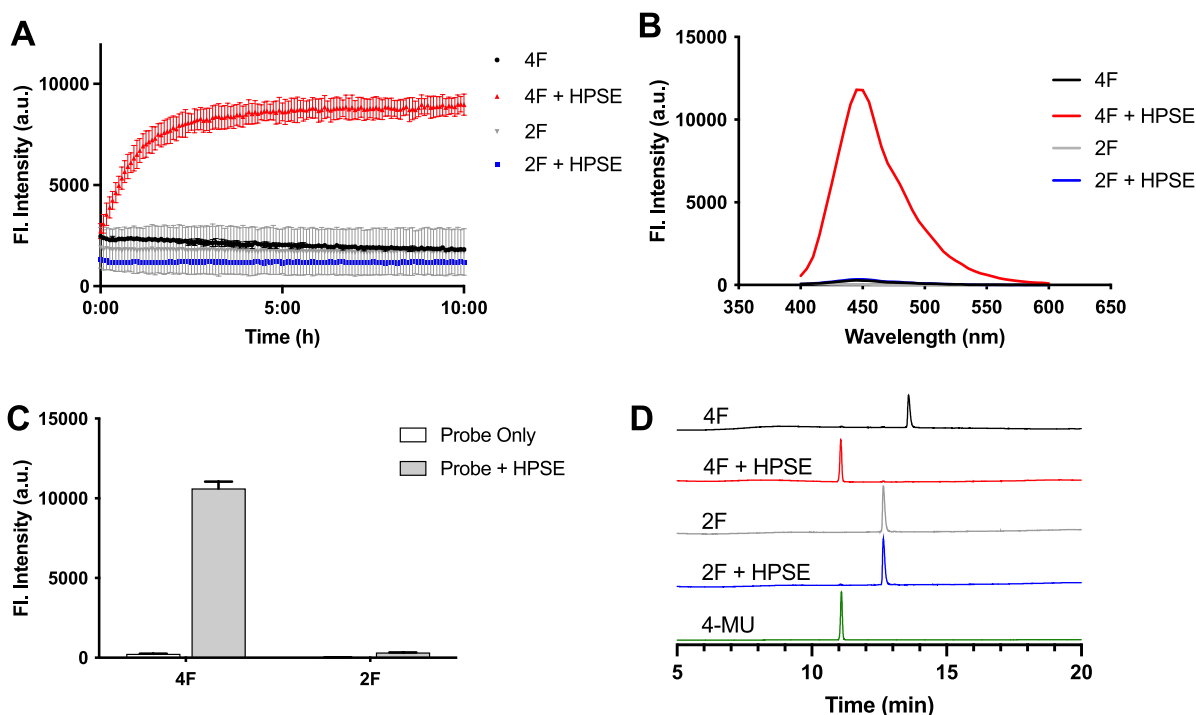


Figure 2. (A) Fluorescence intensity of 2F and 4F incubated with HPSE at pH 5.0. After 22 h, the pH was raised to 7.5 and the emission (B) spectra and (C) intensity at 455 nm was measured. (D) HPLC analysis of probe conversion to the released fluorophore, 4-MU (bottom, green trace) after 22 h.

predicted above, in the design of disaccharide precursors to HADP, the use of the fluorogenic reporter 4-methylumbelliferone (4-MU) did not facilitate turnover of the probe by HPSE, consistent with the exclusive *endo*-glycosidic nature of HPSE enzymatic activity.²¹ However, by incorporating electron-withdrawing fluorine atoms on the 4-MU reporter, *ortho* to the phenolic oxygen, the resulting disaccharide HADP successfully elicited *exo*-glycosidic activity from HPSE.²⁰ To expand the toolkits for HPSE research and medical applications, based on the above-mentioned design strategy (*o,o*-difluorination of the leaving group/reporter), we envisioned that a self-immolative linker with properly tuned electronegativity between the HPSE substrate and the cargo would be more practical and efficient (Figure 1B): in this scheme, the linker would provide the electronic tuning needed for the activation by HPSE, allowing for the incorporation of a cargo by obviating the direct modification on the cargo molecule. This design enables facile incorporation of any cargo ranging from imaging reporters to drugs while streamlining the chemical synthesis of such molecules by providing a single synthetic intermediate for later diversification (compound 10, *vide infra*).

4-Hydroxybenzyl alcohol has been extensively employed as a self-immolative linker in the design of prodrugs, drug delivery systems, sensors, and molecular amplifiers, to bridge the recognition unit and cargo of responsive probes or triggered activation systems.²² Once the recognition unit reacts with the corresponding analyte or biomolecule to free the phenolic hydroxy group, simultaneous elimination occurs to release a molecule of para quinone methide and the cargo (Figure 1B). We incorporated this concept with our previous findings that the addition of electron-withdrawing groups *ortho* to the glycosidic linkage provided a response to HPSE activity via weakening of the glycosidic bond and lowering of the

transition state energy for enzymatic turnover by HPSE.²⁰ Uncertain of the necessary degree of electronic tuning needed to generate HPSE activity with this scaffold, we designed two molecules bearing a 4-hydroxybenzyl alcohol linker substituted with either two or four fluorine atoms to facilitate enzymatic cleavage by HPSE (Figure 1B). To examine our hypothesis that a linker would enable the release of a cargo, 4-MU was used as a fluorescent reporter to allow the detection of a successful response to HPSE activity.

RESULTS AND DISCUSSION

We embarked on the synthesis of compounds 1 (4F) and 2 (2F) (Scheme 1) from disaccharide bromide 3 prepared from commercially available glucosamine and glucose as previously described.²⁰ Reaction under Koenigs-Knorr glycosylation with 4-hydroxybenzaldehyde derivatives 4 and 5, bearing either four or two fluorine atoms, respectively, afforded compounds 6 and 7. The aldehydes were subsequently reduced to the respective primary alcohols 8 and 9, followed by an Appel reaction to create benzyl bromides 10 and 11. A standard S_N2 reaction of fluorobenzyl bromide 10 or 11 with 4-MU in the presence of potassium carbonate to incorporate the fluorescent reporter, established the skeleton of the desired molecules in the form of compounds 12 and 13. Zemplén *O*-deacylation followed by Staudinger reduction of the azido group afforded the respective amines 14 and 15. We note that Pd-catalyzed hydrogenolysis is also a viable method for this azide reduction; however, in some attempts, we observed simultaneous decomposition of the 4-MU moiety (via reduction) as evidenced by a change in HPLC retention time and absorbance spectrum (data not shown). In contrast, Staudinger reduction with PMe_3 provided good yields with no observed side reactions and allowed direct purification by HPLC. From here, saponification of the glucuronic acid

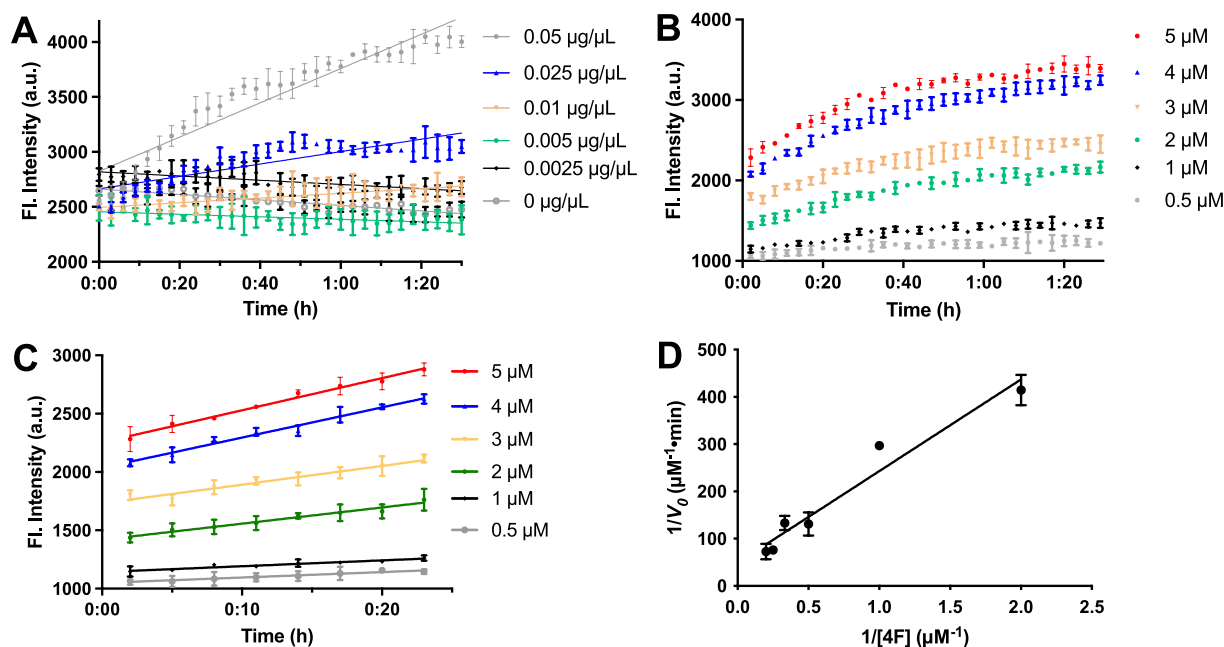


Figure 3. Kinetic analysis of 4F activation by HPSE. Fluorescence intensity in response to varying concentration of (A) HPSE or (B) probe 4F. (C) The initial linear range from panel B, which was used to construct a (D) Lineweaver–Burk plot for 4F.

methyl ester followed by glucosamine *N*-sulfation created compounds **1** and **2**. The final compounds were characterized by HPLC, NMR, and high-resolution ESI-MS (see [Supporting Information](#)).

With the desired compounds in hand, we investigated the enzymatic response of compounds **1** (4F) and **2** (2F) to HPSE in NaOAc buffer (pH 5.0) by measuring the increase in fluorescence emission from the (putatively) released 4-MU reporter ([Figure 2](#)). For compound 2F, no increase in fluorescence was observed after incubation for 22 h, while compound 4F immediately displayed a dramatic fluorescence enhancement ([Figure 2A](#)). Upon completion of the assay, the pH was increased to 7.5 to fully shift the released 4-MU into its highly fluorescent conjugate base form,²³ resulting in a 43-fold increase in fluorescence over the probe background ([Figure 2B,C](#) and [Supplementary Figure S1](#)). The conversion of 4F by HPSE was corroborated by HPLC, giving a single new peak in alignment with that of 4-MU ([Figure 2D](#)). In contrast, the HPLC trace of 2F remained unchanged in the presence of HPSE.

We extracted the kinetics of the reaction between HPSE and probe 4F ([Figure 3](#), [Supplementary Figure S2](#)). The enzyme–substrate pair was measured to have a Michaelis constant (K_M) of 3.97 μM , a catalytic efficiency (k_{cat}/K_M) of 0.06 $\mu\text{M}^{-1}\cdot\text{min}^{-1}$, and a turnover number (k_{cat}) of 0.24 min^{-1} . Compared to our previous probe, HADP, probe 4F exhibits approximately half of the catalytic efficiency (HADP $k_{\text{cat}}/K_M = 0.11 \mu\text{M}^{-1}\cdot\text{min}^{-1}$), one-third of the turnover number (HADP $k_{\text{cat}} = 0.75 \text{min}^{-1}$), and approximately twice the affinity for the enzyme (HADP $K_M = 7.0 \mu\text{M}$). The values determined here between HPSE and HADP ([Supplementary Figure S3](#)) are lower than those in our initial report using HADP;²⁰ this difference likely reflects the batch-to-batch variability in the activity of expressed HPSE protein used in our previous and current reports, a phenomenon also described by other laboratories.¹¹ Nevertheless, all compounds in this report were reacted with the same batch of HPSE, meaning HADP

here serves as a positive control against which 2F and 4F can be compared. Considering the kinetic values determined here, as an exemplary fluorogenic probe, 4F demonstrates a robust response to HPSE. This confirms our hypothesis that a linker with tuned electronegativity will sufficiently reproduce the activity observed for HADP.

To gain a comprehensive understanding of the nature of 4F contributing to this activity, we executed *in silico* experiments to compare probe 4F with inactive compound 2F, probe HADP, and theoretical compound 0F ([Figure 4](#)).

In our previous work, we calculated the glycosidic bond length between the glucuronic acid residue and the fluorophore of HADP, discovering it to be longer than that of the inactive control probes also examined.²⁰ This contributed to our hypothesis that tuning the electronegativity of the aglycone could lead to a slightly lengthened and weakened glycosidic bond that could be activated by HPSE. To further challenge this hypothesis, we performed similar calculations for 2F and 4F using our previous methods and value for HADP as a standard ([Figure 4](#)).²⁰ Notably, the calculated bond length of inactive compound 2F in the presence of the HPSE catalytic dyad²⁴ was slightly shorter than that of active probe HADP ([Figure 4](#)), suggesting a stronger bond more resistant to cleavage by HPSE. On the other hand, the calculated glycosidic bond length of active probe 4F was slightly longer than that of HADP ([Figure 4](#)), suggesting a weaker bond susceptible to cleavage by HPSE. Furthermore, the theoretical compound 0F reported a significantly shorter glycosidic bond compared to the other molecules; this likely reflects the great influence that *o,o*-difluorination has on the phenolic oxygen in these aromatic aglycones, as demonstrated by HADP and related compounds.^{20,25} Still, *o,o*-difluorination of the 4-hydroxy benzyl alcohol linker (2F) provides insufficient tuning for HPSE probes. In the case of HADP, additional electronegativity comes from the electron-withdrawing coumarin ring system, while in the case of 4F this is

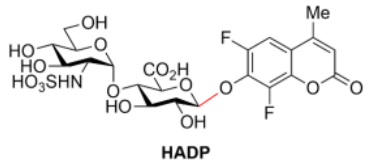
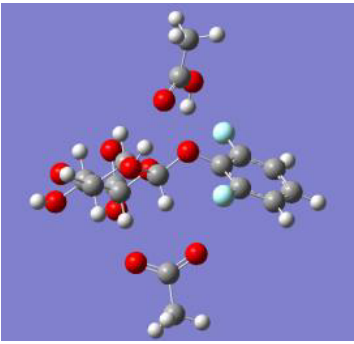
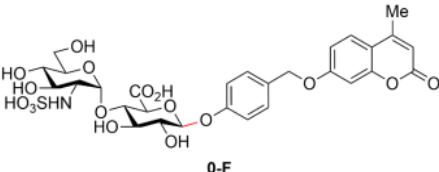
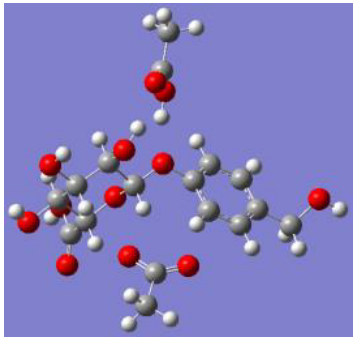
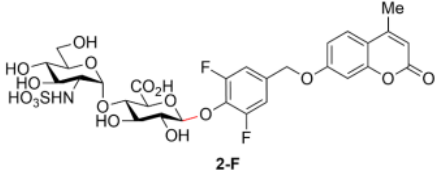
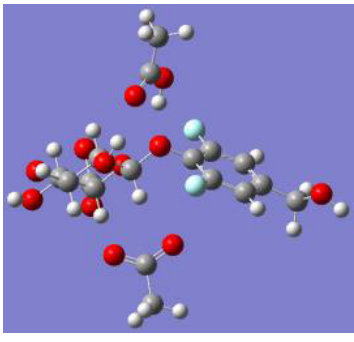
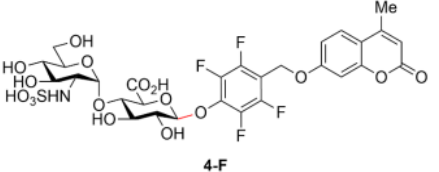
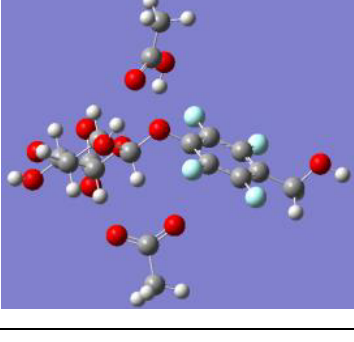
Compounds		$R(\text{C-O})$ /Å
 <p>HADP</p>		1.44093
 <p>0-F</p>		1.42012
 <p>2-F</p>		1.44037
 <p>4-F</p>		1.44370

Figure 4. Calculated glycosidic bond lengths for **2F** and **4F** (and theoretical compound **0F**) in the presence of the HPSE catalytic dyad, standardized against reported probe **HADP**.

accomplished by the further inductive effect provided by the additional two fluorine atoms.

To examine whether the aglycone affects the interaction with heparanase, we performed docking studies of **4F**, **2F**, and theoretical compound **0F** in the HPSE active site, and compared the results to those of **HADP**. For the compounds in this work, the number of fluorine atoms on the benzyl alcohol linker did not affect the binding of the disaccharide

moiety with HPSE. The disaccharide parts of **0F**, **2F**, and **4F** show very similar binding patterns (Figure 5, Movies S1–S3): the 5-carboxylic group interacts with Gly349, Gly350, and Tyr391; the 2'-sulfamic group interacts with Asn64 and Gly389; and, most importantly, the oxygen at the cut site of the molecules shows direct contact with Glu225, the catalytic residue of HPSE.²⁴ This last observation reveals the great cleavable nature of our probes. The hydroxyl groups on the

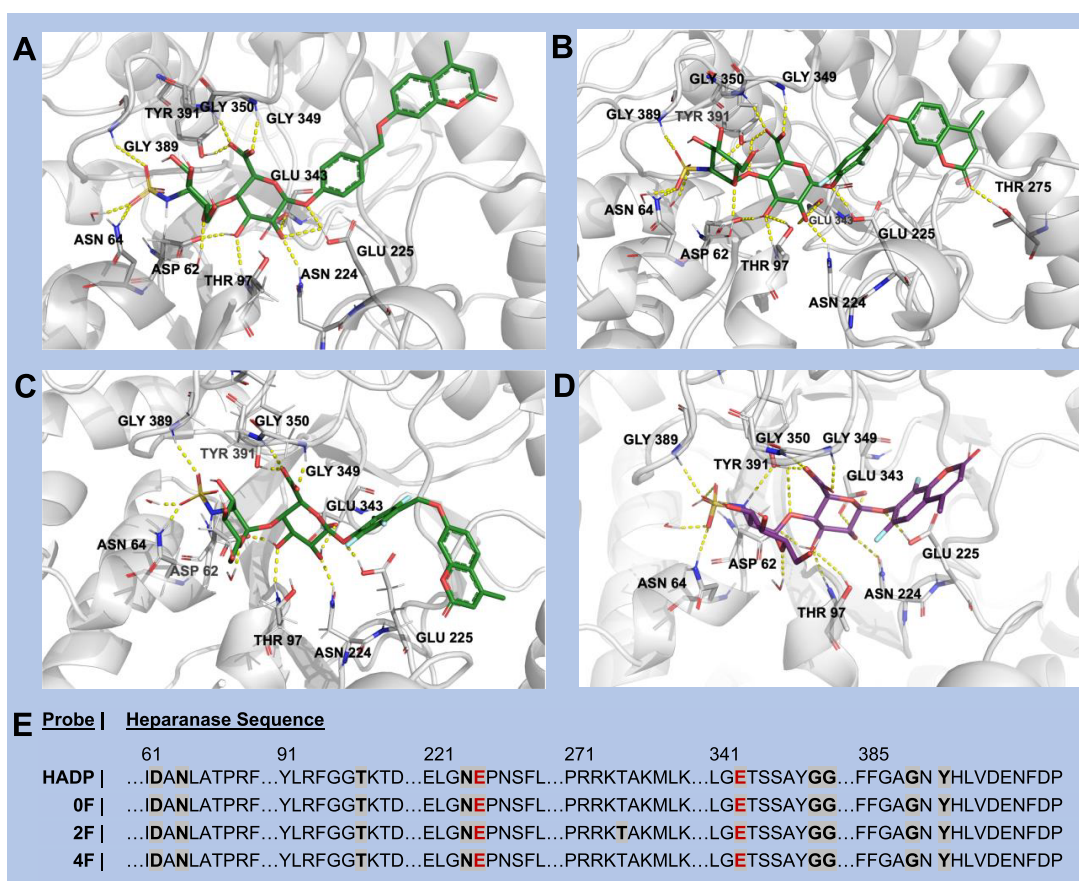


Figure 5. Binding map of (A) **0F**, (B) **2F**, (C) **4F**, and (D) **HADP** with HPSE. (E) The probe/HPSE interactions from the models, within the amino acid sequence of human HPSE.^{2,26} Amino acids interacting with probes are bolded and highlighted. The catalytic dyad is marked in red.

disaccharide also interact with Asp62, Thr97, and Asn224. Interestingly, the disaccharide hydroxyl group close to the hemiacetal group also interacts with Glu343, which is the other catalytic residue of HPSE.²⁴ Aside from the disaccharide, interactions with the other portions of the probes appear negligible: in all cases, the 4-hydroxybenzyl alcohol linker shows no interaction with the HPSE binding pocket. Overall, compounds **0F**, **2F**, and **4F** have nearly identical interactions with HPSE. We then compared the probe/HPSE interactions with those of **HADP** (Figure 5D, Movie S4) to determine if the binding mode would be different. We observed the very same mode of interactions for **HADP** as with probe **4F**, which parallels both probes experiencing turnover by HPSE (Figures 2, 3, and Supplementary Figure S3). To further understand the divergent activities of **2F** and **4F**, Mulliken charges were calculated for the glycosidic bond in each compound and compared to **HADP**. In general, both **2F** and **4F** retained the partial negative charge on the oxygen atom compared to **HADP** while exhibiting a notably larger positive charge on the anomeric carbon (Supplementary Table S1). This increased separation of charge, combined with the greater calculated bond length, explains the activity of **4F** compared to **2F**. Collectively, the data suggest that the substitution of another imaging moiety or cargo for 4-MU will not appreciably affect the activity observed for the tetrafluoro-scaffold examined here, allowing its use as a universal scaffold.

CONCLUSIONS

Attempts to create disaccharide-based HPSE substrate-based probes generally pursue one of two strategies: (i) modify the disaccharide to improve binding and recognition by HPSE, or (ii) modify the aglycone leaving group to adjust the strength of the glycosidic linkage. Strategy (ii) was implemented in this report and proved successful in the creation of probe **4F**, as it did in our development of **HADP** previously.²⁰ In pursuit of strategy (i), the addition of a 6-*O*-sulfate group to the glucosamine residue afforded a probe that was unresponsive in our hands,²⁰ but its slow kinetics were ascertained by others.²⁷ While this probe leverages the known affinity of HPSE for substrates bearing this 6-*O*-sulfate moiety,²⁸ this additional interaction resulted only in a sluggish conversion rate for the probe. Notably, when this 6-*O*-sulfate moiety is absent, the activity of the resulting compound has met with mixed results.^{20,29} Taken together, these studies suggest that adjusting the glycosidic linkage better emulates the conformational changes that occur during HPSE's native *endo*-glycosidase mechanism.²⁸ This conclusion is supported by the docking studies reported here which indicate similar modes of interaction for **0F**, **2F**, **4F**, and **HADP** with HPSE, suggesting this binding arrangement already accommodates enzymatic turnover when paired with a sufficiently tuned glycosidic linkage. Considering the disparate responses of **2F** and **4F** to HPSE, the tetrafluoro-linker may provide this necessary tuning; this likely means that any cargo can be attached for HPSE-directed release, without having to meet any threshold of electron-withdrawing capacity. Similarly, the docking results

show the reporters extending toward the outside of the binding pocket; the linker may allow larger cargo to extend into free space, reducing potential steric hindrance during probe binding.¹⁹ With this in mind, further probe development using the disaccharide tetrafluoro-linker scaffold reported here holds promise. We expect that this disaccharide-linker scaffold will allow access to a variety of new HPSE-responsive imaging probes and drugs enabling the targeting of HPSE in a variety of contexts.

■ ASSOCIATED CONTENT

SI Supporting Information

The Supporting Information is available free of charge at <https://pubs.acs.org/doi/10.1021/acs.bioconjchem.2c00426>.

Additional figures; general experimental, computational, and spectroscopy methods; chemical synthesis protocols with NMR and mass spectrometry characterization (PDF)

Movie of the enzyme/probe docking experiments (Movie S1) (MP4)

Movie of the enzyme/probe docking experiments (Movie S2) (MP4)

Movie of the enzyme/probe docking experiments (Movie S3) (MP4)

Movie of the enzyme/probe docking experiments (Movie S4) (MP4)

■ AUTHOR INFORMATION

Corresponding Author

Lina Cui – Department of Medicinal Chemistry, College of Pharmacy, UF Health Science Center, UF Health Cancer Center, University of Florida, Gainesville, Florida 32610, United States; orcid.org/0000-0002-8149-5206; Email: linacui@cop.ufl.edu

Authors

Kelton A. Schleyer – Department of Medicinal Chemistry, College of Pharmacy, UF Health Science Center, UF Health Cancer Center, University of Florida, Gainesville, Florida 32610, United States

Jun Liu – Department of Medicinal Chemistry, College of Pharmacy, UF Health Science Center, UF Health Cancer Center, University of Florida, Gainesville, Florida 32610, United States

Zixin Chen – Department of Medicinal Chemistry, College of Pharmacy, UF Health Science Center, UF Health Cancer Center, University of Florida, Gainesville, Florida 32610, United States; orcid.org/0000-0001-7441-1353

Zhishen Wang – Department of Medicinal Chemistry, College of Pharmacy, UF Health Science Center, UF Health Cancer Center, University of Florida, Gainesville, Florida 32610, United States

Yuzhao Zhang – Department of Medicinal Chemistry, College of Pharmacy, UF Health Science Center, UF Health Cancer Center, University of Florida, Gainesville, Florida 32610, United States

Junxiang Zuo – Department of Chemistry and Chemical Biology, University of New Mexico, Albuquerque, New Mexico 87131, United States; orcid.org/0000-0002-2967-125X

Alberto Jimenez Ybargollin – Department of Medicinal Chemistry, College of Pharmacy, UF Health Science Center,

UF Health Cancer Center, University of Florida, Gainesville, Florida 32610, United States; orcid.org/0000-0001-7958-7761

Hua Guo – Department of Chemistry and Chemical Biology, University of New Mexico, Albuquerque, New Mexico 87131, United States; orcid.org/0000-0001-9901-053X

Complete contact information is available at:

<https://pubs.acs.org/10.1021/acs.bioconjchem.2c00426>

Author Contributions

#KAS and JL contributed equally to the work. JL and LC designed the project. KAS, JL, and ZW synthesized the compounds, and KAS and JL performed characterization. JL and ZC performed the enzyme assays. AJY expressed the HPSE enzyme. YZ, JZ, and HG performed computational calculations and modeling. KAS, JL, and LC wrote the paper. All authors reviewed the manuscript and provided feedback.

Notes

The authors declare the following competing financial interest(s): The University of Florida has filed a patent on the work.

■ ACKNOWLEDGMENTS

This work is supported by research grants to Prof. L. Cui from the National Institute of General Medical Sciences of the National Institutes of Health (Maximizing Investigators' Research Award for Early Stage Investigators, R35GM124963), the Department of Defense (Congressionally Directed Medical Research Programs Career Development Award, W81XWH-17-1-0529), and to K.A. Schleyer from the University of Florida Health Cancer Center (UFHCC Predoctoral Award). We are grateful for the support from the University of Florida (UF) and the UF Health Cancer Center. NMR spectra were collected from the Department of Medicinal Chemistry, College of Pharmacy, University of Florida (UF). Mass spectrometry services were provided in part by the Mass Spectrometry Research and Education Center, Department of Chemistry, UF (supported by NIH S10 OD021758-01A1). A portion of this work was performed in the McKnight Brain Institute at the National High Magnetic Field Laboratory's Advanced Magnetic Resonance Imaging and Spectroscopy (AMRIS) Facility, which is supported by the National Science Foundation Cooperative Agreement DMR-1644779 and the State of Florida. A portion of this work was carried out using a 1.5 mm High Temperature Superconducting Cryogenic Probe³⁰ developed with support from NIH award R01 EB009772. We are grateful to Jim Rocca, UF AMRIS, for guidance in acquiring NMR data.

■ REFERENCES

- (1) Ilan, N.; Elkin, M.; Vlodavsky, I. Regulation, function and clinical significance of heparanase in cancer metastasis and angiogenesis. *Int. J. Biochem. Cell Biol.* **2006**, *38* (12), 2018–2039.
- (2) Vlodavsky, I.; Friedmann, Y.; Elkin, M.; Aingorn, H.; Atzmon, R.; Ishai-Michaeli, R.; Bitan, M.; Pappo, O.; Peretz, T.; Michal, I.; et al. Mammalian heparanase: gene cloning, expression and function in tumor progression and metastasis. *Nat. Med.* **1999**, *5* (7), 793–802.
- (3) Rivara, S.; Milazzo, F. M.; Giannini, G. Heparanase: a rainbow pharmacological target associated to multiple pathologies including rare diseases. *Future Med. Chem.* **2016**, *8* (6), 647–680.
- (4) Rabelink, T. J.; van den Berg, B. M.; Garsen, M.; Wang, G.; Elkin, M.; van der Vlag, J. Heparanase: roles in cell survival,

extracellular matrix remodelling and the development of kidney disease. *Nat. Rev. Nephrol.* **2017**, *13* (4), 201–212.

(5) Fux, L.; Ilan, N.; Sanderson, R. D.; Vlodavsky, I. Heparanase: busy at the cell surface. *Trends Biochem. Sci.* **2009**, *34* (10), 511–519. Vreys, V.; David, G. Mammalian heparanase: what is the message? *J. Cell Mol. Med.* **2007**, *11* (3), 427–452. Vlodavsky, I.; Goldshmidt, O.; Zcharia, E.; Atzmon, R.; Rangini-Guatta, Z.; Elkin, M.; Peretz, T.; Friedmann, Y. Mammalian heparanase: involvement in cancer metastasis, angiogenesis and normal development. *Semin Cancer Biol.* **2002**, *12* (2), 121–129.

(6) Cohen, E.; Doweck, I.; Naroditsky, I.; Ben-Izhak, O.; Kremer, R.; Best, L. A.; Vlodavsky, I.; Ilan, N. Heparanase is overexpressed in lung cancer and correlates inversely with patient survival. *Cancer* **2008**, *113* (5), 1004–1011.

(7) Li, J. P.; Vlodavsky, I. Heparin, heparan sulfate and heparanase in inflammatory reactions. *Thromb Haemostasis* **2009**, *102* (5), 823–828.

(8) Simeonovic, C. J.; Ziolkowski, A. F.; Wu, Z.; Choong, F. J.; Freeman, C.; Parish, C. R. Heparanase and autoimmune diabetes. *Front Immunol* **2013**, *4*, 471. Ziolkowski, A. F.; Popp, S. K.; Freeman, C.; Parish, C. R.; Simeonovic, C. J. Heparan sulfate and heparanase play key roles in mouse beta cell survival and autoimmune diabetes. *J. Clin Invest* **2012**, *122* (1), 132–141.

(9) Xiang, J.; Lu, M.; Shi, M.; Cheng, X.; Kwakwa, K. A.; Davis, J. L.; Su, X.; Bakewell, S. J.; Zhang, Y.; Fontana, F.; et al. Heparanase Blockade as a Novel Dual-Targeting Therapy for COVID-19. *J. Virol* **2022**, *96* (7), No. e0005722. Chhabra, M.; Doherty, G. G.; See, N. W.; Gandhi, N. S.; Ferro, V. From Cancer to COVID-19: A Perspective on Targeting Heparan Sulfate-Protein Interactions. *Chem. Rec* **2021**, *21* (11), 3087–3101.

(10) McKenzie, E. A. Heparanase: a target for drug discovery in cancer and inflammation. *Br. J. Pharmacol.* **2007**, *151* (1), 1–14. Mohan, C. D.; Hari, S.; Preetham, H. D.; Rangappa, S.; Barash, U.; Ilan, N.; Nayak, S. C.; Gupta, V. K.; Basappa; Vlodavsky, I.; et al. Targeting Heparanase in Cancer: Inhibition by Synthetic, Chemically Modified, and Natural Compounds. *iScience* **2019**, *15*, 360–390. Masola, V.; Zaza, G.; Gambaro, G.; Franchi, M.; Onisto, M. Role of heparanase in tumor progression: Molecular aspects and therapeutic options. *Semin Cancer Biol.* **2020**, *62*, 86–98.

(11) Whitefield, C.; Hong, N.; Mitchell, J. A.; Jackson, C. J. Computational design and experimental characterisation of a stable human heparanase variant. *RSC Chem. Biol.* **2022**, *3* (3), 341–349.

(12) Loka, R. S.; Yu, F.; Sletten, E. T.; Nguyen, H. M. Design, synthesis, and evaluation of heparan sulfate mimicking glycopolymers for inhibiting heparanase activity. *Chem. Commun.* **2017**, *53* (65), 9163–9166. Loka, R. S.; Sletten, E. T.; Barash, U.; Vlodavsky, I.; Nguyen, H. M. Specific Inhibition of Heparanase by a Glycopolymer with Well-Defined Sulfation Pattern Prevents Breast Cancer Metastasis in Mice. *ACS Appl. Mater. Interfaces* **2019**, *11* (1), 244–254.

(13) Chhabra, M.; Ferro, V. The Development of Assays for Heparanase Enzymatic Activity: Towards a Gold Standard. *Molecules* **2018**, *23* (11), 2971.

(14) Sistla, J. C.; Morla, S.; Alabbas, A. B.; Kalathur, R. C.; Sharon, C.; Patel, B. B.; Desai, U. R. Polymeric fluorescent heparin as one-step FRET substrate of human heparanase. *Carbohydr. Polym.* **2019**, *205*, 385–391. Sistla, J. C.; Desai, U. A Robust, One-step FRET Assay for Human Heparanase. *Bio-Protocol* **2019**, *9* (17), e3356–e3367.

(15) Okada, Y.; Yamada, S.; Toyoshima, M.; Dong, J.; Nakajima, M.; Sugahara, K. Structural recognition by recombinant human heparanase that plays critical roles in tumor metastasis. Hierarchical sulfate groups with different effects and the essential target disulfated trisaccharide sequence. *J. Biol. Chem.* **2002**, *277* (45), 42488–42495.

(16) Dulaney, S. B.; Xu, Y.; Wang, P.; Tiruchinapally, G.; Wang, Z.; Kathawa, J.; El-Dakdouki, M. H.; Yang, B.; Liu, J.; Huang, X. Divergent Synthesis of Heparan Sulfate Oligosaccharides. *J. Org. Chem.* **2015**, *80* (24), 12265–12279. Sun, L.; Chopra, P.; Boons, G. J. Modular Synthesis of Heparan Sulfate Oligosaccharides Having N-Acetyl and N-Sulfate Moieties. *J. Org. Chem.* **2020**, *85* (24), 16082–16098. Lu, W.; Zong, C.; Chopra, P.; Pepi, L. E.; Xu, Y.; Amster, I. J.; Liu, J.; Boons, G. J. Controlled Chemoenzymatic Synthesis of

Heparan Sulfate Oligosaccharides. *Angew. Chem., Int. Ed. Engl.* **2018**, *57* (19), 5340–5344.

(17) Chyan, W.; Raines, R. T. Enzyme-Activated Fluorogenic Probes for Live-Cell and in Vivo Imaging. *ACS Chem. Biol.* **2018**, *13* (7), 1810–1823. Fu, Y.; Finney, N. S. Small-molecule fluorescent probes and their design. *RSC Adv.* **2018**, *8* (51), 29051–29061.

(18) Ohmae, M.; Fujita, Y.; Takada, J.; Kimura, S. Synthesis of a Heparan Sulfate Disaccharide Fluoride for Detection of Heparanase Activity. *Chem. Lett.* **2013**, *42* (10), 1168–1169.

(19) Wu, L.; Viola, C. M.; Brzozowski, A. M.; Davies, G. J. Structural characterization of human heparanase reveals insights into substrate recognition. *Nat. Struct. Mol. Biol.* **2015**, *22* (12), 1016–1022.

(20) Liu, J.; Schleyer, K. A.; Bryan, T. L.; Xie, C.; Seabra, G.; Xu, Y.; Kafle, A.; Cui, C.; Wang, Y.; Yin, K.; et al. Ultrasensitive small molecule fluorogenic probe for human heparanase. *Chemical Science* **2021**, *12* (1), 239–246.

(21) Nakajima, M.; Irimura, T.; Di Ferrante, N.; Nicolson, G. L. Metastatic melanoma cell heparanase - characterization of heparan sulfate degradation fragments produced by B16 melanoma endoglycuronidase. *J. Biol. Chem.* **1984**, *259* (4), 2283–2290. Nakajima, M.; Irimura, T.; Nicolson, G. L. Tumor metastasis-associated heparanase (heparan sulfate endoglycosidase) activity in human melanoma cells. *Cancer Letters* **1986**, *31* (3), 277–283.

(22) Yan, J.; Lee, S.; Zhang, A.; Yoon, J. Self-immolative colorimetric, fluorescent and chemiluminescent chemosensors. *Chem. Soc. Rev.* **2018**, *47* (18), 6900–6916. Alouane, A.; Labruere, R.; Le Saux, T.; Schmidt, F.; Jullien, L. Self-immolative spacers: kinetic aspects, structure-property relationships, and applications. *Angew. Chem., Int. Ed.* **2015**, *54* (26), 7492–7509. Chowdhury, M. A.; Moya, I. A.; Bhilocha, S.; McMillan, C. C.; Vigliarolo, B. G.; Zehbe, I.; Phenix, C. P. Prodrug-inspired probes selective to cathepsin B over other cysteine cathepsins. *J. Med. Chem.* **2014**, *57* (14), 6092–6104.

(23) Fink, D. W.; Koehler, W. R. pH Effects on fluorescence of umbelliferone. *Anal. Chem.* **1970**, *42* (9), 990–993. Nagy, N.; Kuipers, H. F.; Frymoyer, A. R.; Ishak, H. D.; Bollyky, J. B.; Wight, T. N.; Bollyky, P. L. 4-methylumbelliferone treatment and hyaluronan inhibition as a therapeutic strategy in inflammation, autoimmunity, and cancer. *Front Immunol* **2015**, *6*, 123. Sun, W.-C.; Gee, K. R.; Haugland, R. P. Synthesis of novel fluorinated coumarins: Excellent UV-light excitable fluorescent dyes. *Bioorg. Med. Chem. Lett.* **1998**, *8* (22), 3107–3110.

(24) Hulett, M. D.; Hornby, J. R.; Ohms, S. J.; Zuegg, J.; Freeman, C.; Gready, J. E.; Parish, C. R. Identification of active-site residues of the pro-metastatic endoglycosidase heparanase. *Biochemistry* **2000**, *39* (51), 15659–15667.

(25) Geng, J.; Zhang, Y.; Gao, Q.; Neumann, K.; Dong, H.; Porter, H.; Potter, M.; Ren, H.; Argyle, D.; Bradley, M. Switching on prodrugs using radiotherapy. *Nat. Chem.* **2021**, *13* (8), 805–810. Zhang, J.; Gao, Y.; Kang, X.; Zhu, Z.; Wang, Z.; Xi, Z.; Yi, L. o,o-Difluorination of aromatic azide yields a fast-response fluorescent probe for H2S detection and for improved bioorthogonal reactions. *Org. Biomol. Chem.* **2017**, *15* (19), 4212–4217. Xie, Y.; Cheng, L.; Gao, Y.; Cai, X.; Yang, X.; Yi, L.; Xi, Z. Tetrafluorination of Aromatic Azide Yields a Highly Efficient Staudinger Reaction: Kinetics and Biolabeling. *Chem. Asian J.* **2018**, *13*, 1791.

(26) Hulett, M. D.; Freeman, C.; Hamdorf, B. J.; Baker, R. T.; Harris, M. J.; Parish, C. R. Cloning of mammalian heparanase, an important enzyme in tumor invasion and metastasis. *Nat. Med.* **1999**, *5* (7), 803–809.

(27) Wu, L.; Wimmer, N.; Davies, G. J.; Ferro, V. Structural insights into heparanase activity using a fluorogenic heparan sulfate disaccharide. *Chem. Commun. (Camb)* **2020**, *56* (89), 13780–13783.

(28) Peterson, S. B.; Liu, J. Unraveling the specificity of heparanase utilizing synthetic substrates. *J. Biol. Chem.* **2010**, *285* (19), 14504–14513. Peterson, S.; Liu, J. Deciphering mode of action of heparanase using structurally defined oligosaccharides. *J. Biol. Chem.* **2012**, *287* (41), 34836–34843.

(29) Pearson, A. G.; Kiefel, M. J.; Ferro, V.; von Itzstein, M. Synthesis of simple heparanase substrates. *Org. Biomol Chem.* **2011**, *9* (12), 4614–4625.

(30) Ramaswamy, V.; Hooker, J. W.; Withers, R. S.; Nast, R. E.; Brey, W. W.; Edison, A. S. Development of a $(1)(3)\text{C}$ -optimized 1.5-mm high temperature superconducting NMR probe. *J. Magn. Reson.* **2013**, *235*, 58–65.

Recommended by ACS

Fluorescent Peptomer Substrates for Differential Degradation by Metalloproteases

Mariah J. Austin, Adrienne M. Rosales, *et al.*

OCTOBER 21, 2022
BIOMACROMOLECULES

READ 

Dynamic Phosphotyrosine-Dependent Signaling Profiling in Living Cells by Two-Dimensional Proximity Proteomics

Qian Kong, Ruijun Tian, *et al.*

OCTOBER 24, 2022
JOURNAL OF PROTEOME RESEARCH

READ 

An Integrated Proteomic Strategy to Identify SHP2 Substrates

Peipei Zhu, W. Andy Tao, *et al.*

SEPTEMBER 14, 2022
JOURNAL OF PROTEOME RESEARCH

READ 

Middle-Down Mass Spectrometry Reveals Activity-Modifying Phosphorylation Barcode in a Class C G Protein-Coupled Receptor

Ashley N. Ives, Reza Vafabakhsh, *et al.*

DECEMBER 07, 2022
JOURNAL OF THE AMERICAN CHEMICAL SOCIETY

READ 

Get More Suggestions >